High-Resolution Kinetic Studies of the Reassembly of the Tetra-Manganese Cluster of Photosynthetic Water Oxidation: Proton Equilibrium, Cations, and Electrostatics†

Gennady M. Ananyev and G. Charles Dismukes*

Hoyt Laboratory, Department of Chemistry, Princeton University, Princeton, New Jersey 08544

Received April 15, 1996; Revised Manuscript Received September 9, 1996⊗

ABSTRACT: The kinetics of pulsed-light photoactivation, the light-induced reassembly of the water-oxidizing complex (WOC) of PSII in the presence of essential inorganic cofactors, has been studied using two improvements: a new efficient chelator, *N,N,N′,N′*-tetrapropionato-1,3-bis(aminomethyl)benzene (TPDBA), for complete extraction of {Mn_4} and Ca^{2+} and an ultrasensitive polarographic cell for O_2 detection [Ananyev, G. M., & Dismukes, G. C. (1996) *Biochemistry 35*, 4102−4109]. Measurements have been made of the initial half-time, $t_{1/2}$ (sum of the lag time for formation of the first intermediate, IM_1, plus the half-time for formation of the second intermediate, IM_2), and the steady-state yield, Y_{ss}, for recovery of O_2 evolution (proportional to the number of active centers). The following conclusions have been reached: (1) cations (Ca^{2+}, Mg^{2+}, and Na^+) slow the rate of photoactivation, even though Ca^{2+} is essential for activity. Two distinct mechanisms appear to be involved: binding to one or both of the first two Mn^{2+}-specific sites and screening of negative charges on apo-WOC that are responsible for concentrating Mn^{2+} ions by electrostatic steering; (2) the Michaelis constant for the calcium requirement for Y_{ss} at sufficiently low Mn^{2+} concentrations (8 μM) that competition at the calcium site does not occur is K_m = 1.4 mM. Numerically, K_m is the same for reactivation of O_2 evolution in Ca-depleted PSII membranes which retain four Mn ions; (3) in the absence of Ca^{2+} but in the presence of saturating amounts of Mn^{2+} (8 Mn/apo-WOC) and Cl^- (35 mM) assembly of a stable tetra-Mn cluster occurs neither under illumination nor in the dark after subsequent addition of $CaCl_2$. However, in the presence of suboptimal concentrations of calcium required for maximum Y_{ss}, calcium-dependent assembly of stable yet inactive clusters occurs in the light; (4) protons in equilibrium with the buffer greatly increase the half-time 3-fold between pH 6.75 and 5.4, indicating ionization of one or more protons from the first photo-oxidized intermediate formed prior to the rate-limiting step (photo-oxidation of the second Mn^{2+}); (5) the lipophilic membrane soluble anion tetraphenylboron (TPB^-), a known reductant of intact WOC, increases the half-time 2.5-fold ($\leq$40 μM) and paradoxically stimulates Y_{ss} by 50% at 20 μM concentration. These results suggest that TPB^- increases the local concentration of Mn^{2+} adjacent to apo-WOC (Y_{ss} increase), while also reducing the S_2 and S_3 states of the intact WOC at higher concentrations ($t_{1/2}$ increase). The effects of anions and cations indicates that overcoming the surface potential of the membrane/protein PSII complex may play an important role in the kinetics of reassembly of the {Mn_4} cluster; (6) the ratio Y_4/Y_3 in the kinetics of O_2 evolution from a series of single-turnover flashes, a ratio that typically reflects the probability of misses (α), grows noticeably larger with increasing extent of recovery of O_2 evolving activity and also with increase in the amount of Mn^{2+}, indicating competition between substrate water and excess Mn^{2+} for reduction of the functional {Mn_4} cluster. On the basis of these results, we extend the model for photoactivation to include the antagonistic effects of H^+ and Ca^{2+} in the formation of the first two intermediates.

Unlike several stable inorganic clusters observed in biology which undergo spontaneous self-assembly, the WOC[1] possesses an intrinsically unstable core. The tetra-Mn-Ca active center of the WOC of PSII can be reversibly reassembled only in the presence of the apo-PSII membrane/protein complex by a light-driven process called photoactivation (Radmer & Cheniae, 1977; Cheniae, 1980). A few kinetic models for the photoactivation process have been proposed, all in agreement on the formation of a metastable intermediate in the rate-limiting step which requires Mn^{2+} and both light and dark steps to reach (Radmer & Cheniae, 1971; Tamura & Cheniae, 1987; Tamura et al., 1989; Miller & Brudvig, 1989; Blubaugh & Cheniae, 1992). However, supporting evidence that would identify the molecular structures, oxidation states, and chemical reactivities of the proposed intermediates is very limited.

On the basis of steady-state kinetic and biochemical studies Cheniae's group (Tamura & Cheniae, 1987; Blubaugh &

† This work was supported by the National Institutes of Health (Grant GM39932).

* To whom correspondence should be addressed. FAX: (609) 258-1980. E-mail: dismukes@chemvax.princeton.edu.

⊗ Abstract published in *Advance ACS Abstracts,* October 15, 1996.

[1] Abbreviations: Chl, chlorophyll; Bis-Tris, bis(2-hydroxyethyl)-iminotris(hydroxymethyl)methane; LED, light-emitting diode; MOPS, 3-(*N*-morpholino)propanesulfonic acid; MES, 2-(*N*-morpholino)ethanesulfonic acid; P680, primary electron donor; PSII, photosystem II; Pheo, primary pheophytine electron acceptor of PSII; Q_A and Q_B, primary and secondary plastoquinone electron acceptors; RC, reaction center; $t_{1/2}$, half-time kinetics of pulsed-light photoactivation of O_2 evolution; TPB, tetraphenylboron; TPDBA, *N,N,N′,N′*-tetrapropionato-1,3-bis-(aminomethyl)benzene; V_{O_2}, maximal rate of O_2 evolution at saturated continuous light after pulsed-light activation; Y_{ss}, steady-state level kinetics of pulsed-light photoactivation of O_2 evolution; Y_z, redox-active tyrosine-161 of the D1 polypeptide; WOC, water-oxidizing complex.

S0006-2960(96)00894-X CCC: $12.00

Cheniae, 1992) has proposed a two-quantum model for the photoactivation mechanism. Starting from the apo-S-state PSII complex, a two-quantum process occurs in which two Mn^{2+} are sequentially bound, photooxidized, and further ligated to form the rate-limiting unstable intermediate separated by a dark rearrangement step. This process enables the binding of two additional Mn^{2+} ions to form the tetra-Mn S-state complex, by a poorly characterized process involving additional photons and calcium. On the basis of double-flash experiments it was shown that incorporation of Mn^{2+} ions into the apo-WOC center to form and stabilize the rate-limiting intermediate ($t_{1/2}$ = 100 ms) requires the accumulation of at least two positive charges (Ananyev et al., 1988; Klimov et al., 1990). Miller and Brudvig (1990) also concluded from steady-state O_2 kinetics that the first stable intermediate in the assembly of the $\{Mn_4\}$ complex contains Mn^{3+} and hypothesized that the second intermediate could contain a binuclear $Mn^{2+}Mn^{3+}$ center, which is photooxidized to $Mn^{3+}Mn^{3+}$. Recently, we have shown using EPR spectroscopy evidence for binding of two Mn(II) ions in the dark to apo-WOC to form a spin-coupled binuclear Mn_2(II,II) species which can be bleached by light and competed by other divalent cations (Ananyev & Dismukes, 1995). In addition, it was found that at limiting levels of Mn^{2+} the first direct kinetic evidence for formation of a pre-steady-state intermediate (IM_1) involves uptake and photooxidation of a single Mn^{2+} to the apo-WOC (Ananyev & Dismukes, 1996).

Multiple changes accompany the photoactivation process, indicating recovery of normal functioning, including (1) restoration of the S_2-state multiline EPR signal for the intact tetra-Mn-Ca cluster (Miyao-Tokutomi et al., 1990; Miyao & Inoue, 1991); (2) recovery of photoreducible Pheo, Q_A, and DCIP; (3) release of H^+ from substrate water (Klimov et al., 1986, 1987); and (4) restoration of the period-4 oscillatory pattern of thermoluminescence B-band emission from $S_2Q_B^-$ (Tamura & Cheniae, 1988). Also, more than half of the low-potential (LP) form of Cyt b_{559} is converted in the presence of 50 mM Ca^{2+} to the high-potential (HP) form, although the rate of recovery is much faster (5 min) vs the recovery of O_2 evolution (20 min) (Mizusawa & Yamashita, 1992, 1995; Mizusawa et al., 1995). During photoactivation the midpoint potential of Q_A/Q_A^- shifts from +110 to −80 mV, indicating a long-range allosteric coupling of the WOC to Q_A across the thylakoid membrane (Johnson et al., 1995).

Recent studies of Ca^{2+} binding using ^{45}Ca has shown that a single Ca^{2+} ion is required for O_2 evolution (Ädelroth et al., 1995). PSII membrane fragments depleted of the extrinsic 17-, 23-, and 33-kDa proteins, but which retain the tetra-Mn cluster of WOC, can be reactivated in the presence of Ca^{2+} and Cl^- using 100−150 xenon flashes. Photoactivation of the apo-WOC requires the photoinduced uptake of Ca^{2+} ions from the medium (Ananyev et al., 1988). Recent results (Chen et al., 1995) indicate that Ca^{2+} increases the yield of photoactivation by suppressing the extent of photoinactivation caused by inappropriately bound $Mn^{\geq 3}$.

There are some data and much controversy about the proximity of Ca^{2+} to the tetra-Mn cluster. Either a close proximity or protein-mediated conformational coupling of Ca^{2+} to the Mn cluster can be inferred from transformation of the multiline EPR signal upon Ca^{2+} removal (Boussac & Rutherford, 1988, 1989; Sivaraja et al., 1989), replacement of Ca^{2+} by Sr^{2+} (Boussac et al., 1988) and from changes in the Mn EXAFS (Yachandra et al., 1993; Latimer et al., 1995) and FTIR spectroscopy (Noguchi et al., 1995) data. However, Riggs-Gelasco et al. (1995) did not see a change in the 3.3 Å shell in the Mn EXAFS scattering after replacement of Ca(II) with Sr(II), Dy(III), or La(III), which has been partly attributed to a Mn-Ca interaction (Yachandra et al., 1993). Moreover, Tb^{3+} can displace Ca^{2+} from its binding site in the WOC without prior depletion of the cation. The Mn-cluster of the Tb^{3+}-substituted preparations remains structurally intact, can advance to the S_2-state, and exhibits no change in the Mn EXAFS indicating that calcium should be located no closer than 3.6 Å (Hatch et al., 1995).

The competition between Mn^{2+} and other cations, including Ca^{2+}, Mg^{2+}, and Na^+, during photoactivation has been noted previously in earlier models [Ono & Inoue, 1983; Miller & Brudvig, 1989; for review see Yocum (1991)]. Divalent cations suppress reoxidation of reduced DCIP by Mn^{3+} formed during photoactivation with the following hierarchy: $Ca^{2+} > Sr^{2+} > Ba^{2+} \gg Mg^{2+}$ (Tamura & Cheniae, 1988). This result suggests that calcium and possibly the heavier alkaline earth ions interact with an early photoproduct in the photoactivation process to kinetically or thermodynamically stabilize it from reacting with exogenous reductants. These data are consistent with the "gatekeeper" role for Ca^{2+} that has been proposed in protecting the WOC against hydrolysis by limiting accessibility of water to exclusively two substrate molecules (Tso et al., 1991).

In the present article we further analyze the kinetics of photoactivation, i.e., the time course for recovery of flash-induced O_2 yield, using the aforementioned technical improvements (Ananyev & Dismukes, 1995, 1996). Here we report data on the critical role played by protons and on the competition between Ca^{2+}, Mg^{2+}, and Na^+ for uptake of Mn^{2+}. We use these data to extend Cheniae and Tamura's model for photoactivation. By examining the influence of Ca^{2+} on photoactivation at Mn^{2+} concentrations that are ~250 times less than those reported in the literature, we are able to examine the role of calcium under conditions where Mn^{2+} does not effectively compete with the calcium site or other divalent ion sites. We find that Ca^{2+} ions are required not only for catalysis of water oxidation to yield O_2 but also for assembly of the stable tetra-Mn cluster during photoactivation. We also report new data demonstrating that the miss parameter, α, in the S_0-S_4 cycle of O_2 evolution is markedly increased during photoactivation.

MATERIALS AND METHODS

PSII enriched membrane fragments (BBY) were prepared from market spinach using the method of Berthold et al. (1981) with some minor modifications (Ghanotakis et al., 1984). Samples (at 1 mg of Chl per mL) were stored in 10% glycerol at −196 °C until they were slowly thawed and washed once in a medium containing 300 mM sucrose, 35 mM NaCl, 25 mM MES/NaOH buffer (pH 6.0) (assay medium). The oxygen evolution rate under saturated continuous illumination of the untreated PSII membrane fragments with 0.8 mM K_3FeCN_6/1.2 mM DCBQ as electron acceptors was 400−500 μmol of O_2/(mg of Chl h). The concentration of the RC PSII was measured from the photoinduced absorption changes of Pheo at 685 nm with the extinction coefficient $\epsilon = 0.32 \times 10^5\ M^{-1}\ cm^{-1}$ (Klimov et al., 1982).

Manganese and calcium were removed from PSII membrane fragments (0.25−1.0 mg of Chl/mL) using the normal assay medium along with 25−35 mM TPDBA and 1 mM ascorbate, as described earlier (Ananyev & Dismukes, 1995, 1996).

Photoactivation of TPDBA-depleted PSII membranes (apo-WOC) by light pulses and polarographic detection of O_2 in the assay medium containing 0.8 mM K_3FeCN_6 were performed simultaneously in a Clark-type microcell of 5 μL volume covered with a silicone or FUM (Russia) membrane capable of 100 ms time resolution (Ananyev & Dismukes, 1996). Home-made silicone membranes with less than 5 μm thickness were prepared from the rubber adhesive sealant Translucent RTV 108 (General Electric). A flat glass plate with dimensions 100 × 73 × 1 mm^3 was covered by a 25 mm wide and 20 μm thick Teflon film. Scotch tape with thickness 25−50 μm was attached on both sides of Teflon tape in order to form a cavity for membrane 5−30 μm high. A small amount of silicone sealant was slowly and uniformly spread on the Teflon surface between the Scotch tape strips using a small glass rod. Polymerization of the silicone membrane was performed at room temperature for 1 h and at 70 °C for another 1 h for complete evaporation of acetic acid.

The amplified signal from a precision low-noise current-to-voltage converter and amplifier with adjustable high- and low-frequency filters (model 113 low-noise preamplifier, EG&G Princeton Applied Research Corp.) was digitized by DI-200 12-bit data acquisition interface with WinDaq data acquisition and waveform analysis software for Windows (computer IBM PC350-100DX4). The sensitivity enables detection of ~5 × 10^{-14} mol of O_2 per flash.

Description of the pulsed LED microcell used for photoactivation is given elsewhere (Ananyev & Dismukes, 1995, 1996). Flash O_2 measurements were performed in the presence of an artificial acceptor of electrons using the same silicone-membrane covered O_2-microcell equipped with a xenon flash lamp (4 μs FWHM and 0.3 Hz frequency).

RESULTS

Dependence of Y_{ss} and $t_{1/2}$ on Ca^{2+}, Mg^{2+}, and Na^+. It was established in earlier work that calcium is essential for photoactivation. However, its presence is known to delay the rate of recovery of O_2 evolution. This phenomenon is shown in Figure 1A, depicting the increase in the final steady-state yield (Y_{ss}) and the decrease in half-time for photoactivation with increasing concentration of $CaCl_2$, at low Mn^{2+} concentrations which do not interfere. The half-time increases by 10-fold (from 1 to 10 min) in the concentration range between 1 and 40 mM $CaCl_2$. Neither $MgCl_2$ nor NaCl supports photoactivation alone, but in the presence of Ca^{2+} sufficient to support O_2 activity, both slow the rate of photoactivation (Figure 1B,C). Both Mg^{2+} and Na^+ exert relatively weak retardation of the rate of photoactivation. The initial slopes of the plots of half-time versus salt concentration give the relative effectiveness for slowing the photoactivation process (named as symbol "*A*"): A_{Ca} = 13 s/mM, A_{Mg} = 4.7 s/mM, and A_{Na} = 0.14 s/mM.

In our experiments only $CaCl_2$ causes an increase in Y_{ss} with a Michaelis constant of K_m = 1.4 mM, very similar to the range 1−1.3 mM previously reported (Boussac at al., 1986; Chen et al., 1995). Addition of $MgCl_2$ at a fixed

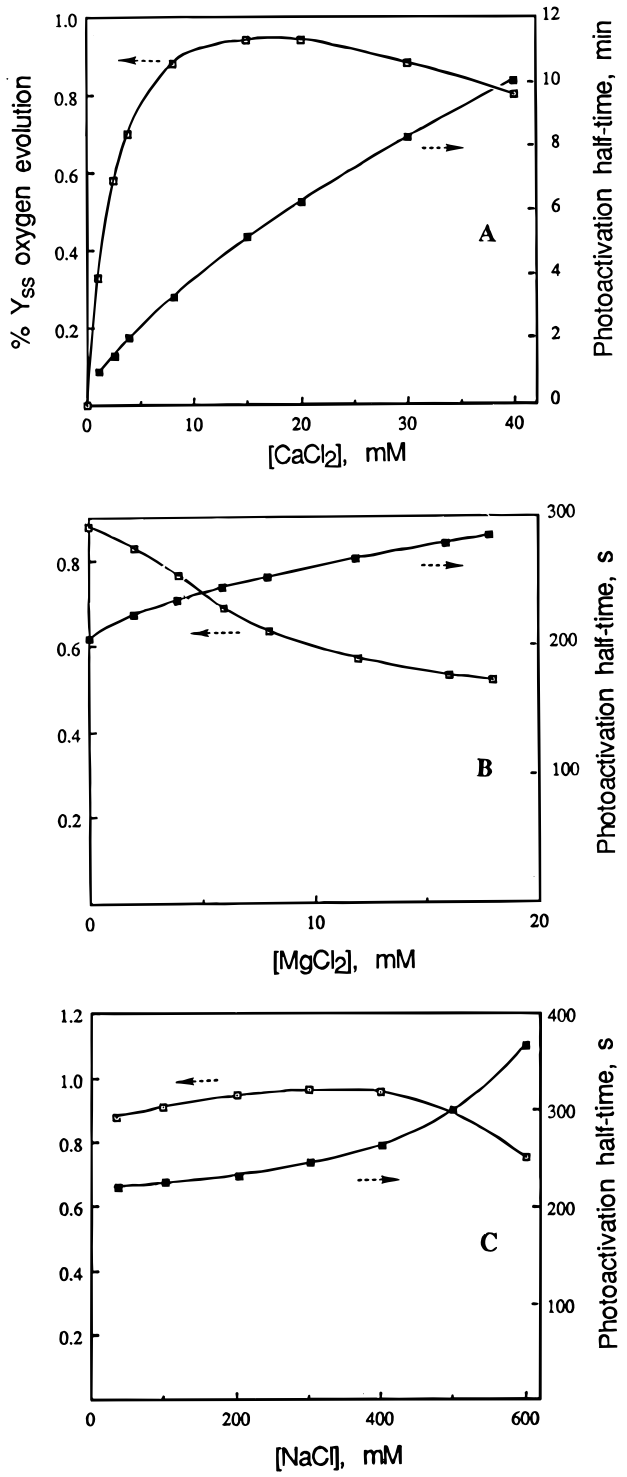

FIGURE 1: Dependence of the recovery of photoactivation yield, Y_{ss}, and half-time, $t_{1/2}$, on the concentration of $CaCl_2$ (A), $MgCl_2$ (B), and NaCl (C). The plots for $MgCl_2$ and NaCl were obtained at a fixed concentration of $CaCl_2$ equal to 8 mM. Data points are calculated from pulsed-light kinetics of O_2 evolution after attaining the steady-state level Y_{ss}. Assay conditions: apo-PSII membranes extracted with TPDBA (1 μM RC PSII), 25 mM MES/NaOH buffer (pH 6.0), 35 mM NaCl, 300 mM sucrose, 0.8 mM K_3FeCN_6, 8 μM $MnCl_2$, 8 mM $CaCl_2$. Photoactivation conditions: t_{light} = 40 ms, t_{dark} = 2 s, total time of pulsed-light illumination 15 min, I_p = 80 mW/cm^2, λ_{max} = 660 nm. Y_{ss} is reported as percent of O_2 evolution rate of untreated PSII membranes with 0.8 mM K_3FeCN_6 as an electron acceptor. The absolute rate is equal to 280 μmol of O_2/mg of Chl h. Thus, 1% Y_{ss} on *Y*-scale corresponds to about 2.8 μmol of O_2/(mg of Chl h).

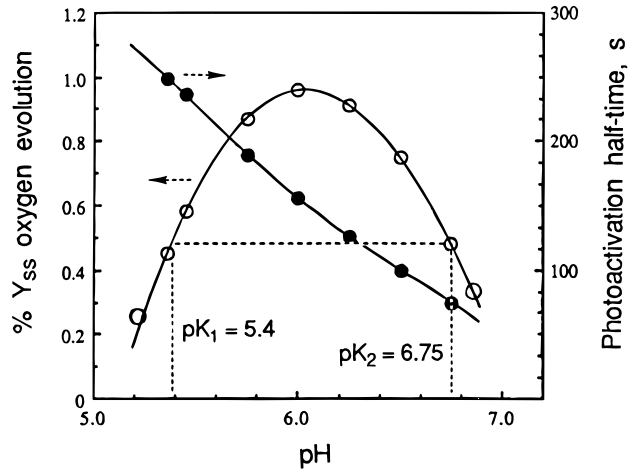

FIGURE 2: Effect of pH on Y_{ss} and half-time, $t_{1/2}$, for photoactivation of apo-WOC. The assay conditions were as in Figure 1.

concentration of $CaCl_2$ (8 mM) decreases the maximum level of Y_{ss} by 35% at 18 mM $MgCl_2$ and not at all in the case of NaCl up to 0.4 M. Thus, we can conclude that both Mg^{2+} and particularly Ca^{2+} slow the kinetics of the rate-limiting process in photoactivation or shift it to another slower step and that Mg^{2+} also lowers the yield of activated centers. We have shown previously that formation of the second intermediate represents the rate-limiting process in the absence of Mg^{2+}. On the other hand, Na^+ exerts only minor effects except above 0.4 M where ionic strength effects become an issue. The slower rates of photoactivation seen with increasing concentrations of Ca^{2+} and Mg^{2+} can be overcome by increasing the Mn^{2+} concentration (a detailed study separating the effects on the first and second intermediates is in progress). Thus, the alkaline earth ions appear to compete with Mn^{2+} binding, although it is unclear on the basis of kinetics alone if this competition occurs directly at the high-affinity Mn site where binding and photooxidation occur ($K_m \approx 1\ \mu$M) or at lower-affinity sites that are conformationally coupled to the first or second Mn site.

Role of Protons in Photoactivation. The pH dependence of the yield of photoactivation exhibits a parabolic curve with maximum at pH 6.0 and 50% inhibition points corresponding to apparent ionization sites with pK_1 = 5.4 and pK_2 = 6.75 (Figure 2). This classic type curve is commonly associated with two types of functional groups involved in proton equilibrium, in this case coupled to assembly or activity of the WOC. The pH maximum of the steady-state O_2 evolution rate in PSII particles under saturating red light is well-known to exhibit a much wider pH range for optimal activity (Vass & Styring, 1991), suggesting that the pH dependence of Y_{ss} reflects primarily the pK_a of functional groups associated with the assembly process and not the acceptor side.

Figure 2 also shows that the photoactivation half-time decreases by 3-fold uniformly from 250 to 80 s with increasing pH over this same range from pH 5.4 to 6.75. The average slope over this interval is A_{H^+} = 120 s/pH unit. Hence, in contrast to the yield data, the half-time indicates only a single type of species whose deprotonation is required to allow formation of the rate-limiting species. The pK_a of this site must be below 5.4 in order to explain the monotonic increase in the half-time in the observed pH range.

In order to better understand the chemical origin of this deprotonation reaction required for formation of the rate-determining intermediate, Y_{ss} and $t_{1/2}$ were measured as a function of the buffer concentration in the range 1.5−100 mM MES/NaOH at pH 6.00 (Figure 3). We found a strong dependence of Y_{ss} and a weak dependence of $t_{1/2}$ on the buffer concentration characterized as follows: (1) the maximum Y_{ss} is reached at 12−25 mM MES with 50% loss of Y_{ss} observed at 3 mM MES and 11% loss at 100 mM MES; (2) $t_{1/2}$ increases by only 20% from 140 to 170 s with increasing concentration of MES between 1.5 and 50 mM, and weak acceleration by 11% at 100 mM MES.

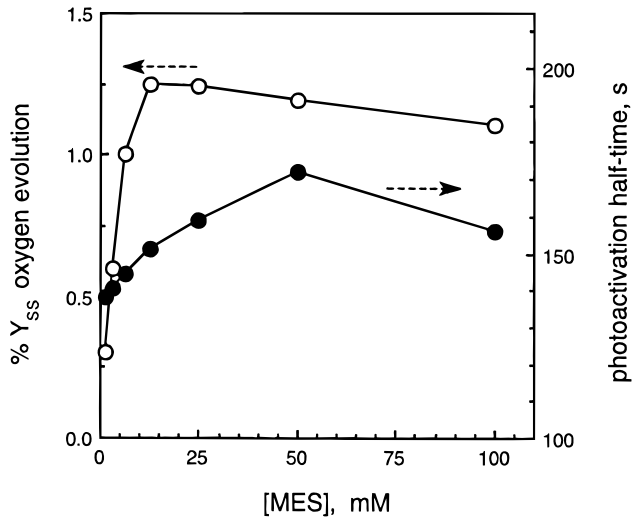

FIGURE 3: Dependence of the yield, Y_{ss}, and the half-time, $t_{1/2}$, for photoactivation on the concentration of MES-buffer of stock solution. The assay contained 8 μM Mn^{2+}, 8 mM $CaCl_2$, 35 mM NaCl, 300 mM sucrose, and 250 μg of Chl per mL. The conditions of pulsed-light illumination are as follows: t_{light} = 30 ms, t_{dark} = 2 s.

Comparison of the effects of different organic buffers on the assembly process shows that when 25 mM MOPS buffer (pK_a = 7.20) was used instead of 25 mM MES buffer (pK_a = 6.15) in the assay medium at the same pH of 6.5, the level of Y_{ss} was suppressed by 50% but $t_{1/2}$ was not changed. On the other hand, complete removal of {Mn_4} using an assay medium containing 25 mM MOPS buffer required that the concentration of TPDBA be increased from 25 to 30 mM, in comparison to the same procedure in 25 mM MES buffer. So, MOPS buffer better protects manganese in the WOC from extraction by TPDBA. In the assay medium with 25 mM Bis-Tris buffer (pK_a = 6.80) at the same pH of 6.5 the yield Y_{ss} was fully inhibited. However, oxygen evolution by untreated PSII fragments in the assay medium with 25 mM Bis-Tris buffer (pH 6.5) was inhibited only by 60% vs MES buffer. Possibly weak association of Mn^{2+} by the MOPS and Bis-Tris decreases the thermodynamic activity of Mn^{2+} in solution. This buffer effect on Y_{ss} may indicate that the availability of a proton acceptor at the photoactivation site may differ for these buffers, perhaps due to different accessibilities or differential screening effects from charge. The lack of an effect on $t_{1/2}$ of the different buffers indicates that the rate-limiting step does not involve release of a proton into solution.

Lipophilic Membrane Permeable Ions TPB^- and TPP^+. In order to obtain more information about the role of surface potential (Itoh et al., 1983) of PSII membrane fragments in the photoassembly of the WOC we studied the effect of low concentrations of the lipid soluble ions. The anion tetraphenylboron, TPB^-, partitions into phospholipid membranes

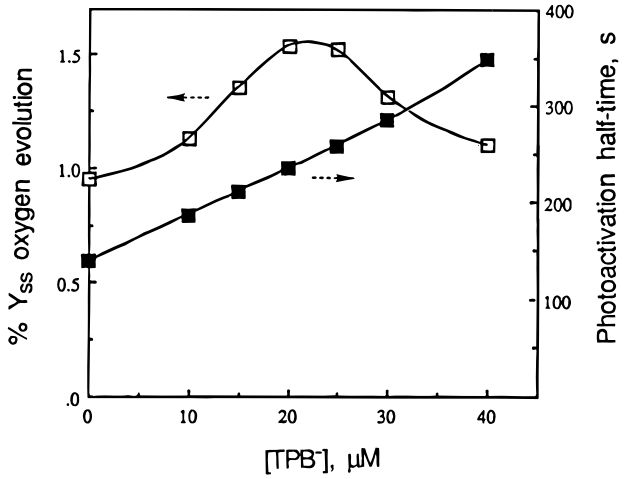

FIGURE 4: Effect of the lipid soluble anion tetraphenylboron (TPB^-) on Y_{ss} and $t_{1/2}$ for pulsed-light photoactivation of apo-PSII membranes. The assay and photoactivation conditions were as in Figure 1.

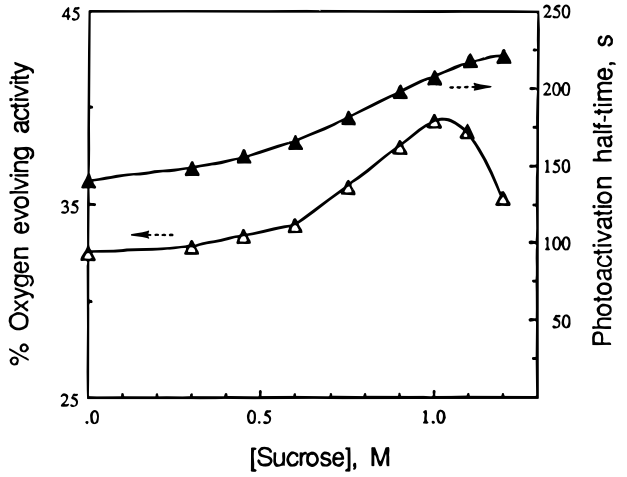

FIGURE 5: Dependence on the concentration of sucrose of $t_{1/2}$ and maximal rate of O_2 evolution (V_{O_2}) at saturated continuous light after pulsed-light photoactivation for apo-PSII membranes. The assay and photoactivation conditions were as in Figure 1.

from aqueous media, reaching a maximum equilibrium concentration of 1.5×10^{12} molecules/cm^2 or roughly 1 per 100 phospholipid molecules (the binding constant, defined as the ratio of bound to free TPB^-, is 10^5-10^6). TPB^- probably shifts the surface potential to a more negative value in the protein−lipid complex of PSII. Addition of TPB^- from 0 to 40 μM (Figure 4) results in a 2.5-fold increase in $t_{1/2}$ with mean slope $A_{TPB^-} = 4.5$ s/μM, while the yield Y_{ss} is stimulated by 50% at 20 μM TPB^-.

The lipid soluble cation tetraphenylphosphonium, TPP^+, binds 10^3-10^4 times more weakly to lipid bilayers than TPB^-, with a binding constant of 10^2. In contrast to TPB^-, addition of TPP^+ (40 μM) has no effect on the kinetics of recovery of photoactivation, on neither Y_{ss} nor $t_{1/2}$ (data not shown). Addition of TPP^+ to intact PSII membranes had no effect on the steady-state rate of O_2 evolution (data not shown). Millimolar and higher concentrations could not be studied owing to insolubility of TPP^+ in aqueous buffer. Hence, the concentration range where partitioning into the PSII membrane would yield a comparable membrane-bound concentration as with TPB^- could not be explored.

These results suggest that the surface potential of PSII membranes plays an important role in the kinetics of reassembly. The stimulating effect of TPB^- on Y_{ss} peaking at 20 μM concentration could be due to an increase in the local concentration of Mn^{2+} near PSII membranes, owing to the higher negative charge which accumulates on the membrane in the presence of TPB^-. In support of this proposal, we find that in the absence of TPB^- increasing the Mn concentration in solution accelerates the rate of the rate-limiting step in photoactivation by a first-order process (proportional to $[Mn]^1$) (Ananyev & Dismukes, 1995, 1996). The origin of the increase in $t_{1/2}$ observed with TPB^- can be ascribed to reduction of either one or both of the initial photointermediates. TPB^- can be oxidized irreversibly to a radical form at a reduction potential of $E_m = +550$ mV vs NHE (0.15 M tetrabutylammonium perchlorate in acetonitrile). TPB^- is known to reduce both the S_2 and S_3 states of the intact WOC and also tyrosine Y_z^+ (Erixon & Renger, 1974; Khanna et al., 1981; Tamura & Cheniae, 1987). TPP^+ has no effect on $t_{1/2}$ ($\leq$40 μM), and this is consistent with it not being capable of reducing Y_z^+ or the S_i states. An alternative interpretation for the increase in Y_{ss} by TPB^- may be to reductively eliminate nonfunctional Mn which reduces the yield of photoactivation at excess Mn concentrations (Chen et al., 1995). However, this proposed mechanism could not be operating in our experiments which were conducted at low Mn concentrations where nonfunctional Mn does not interfere, i.e., where Y_{ss} is independent of the Mn concentration.

Effect of Osmolytes on Y_{ss} and $t_{1/2}$. Osmolytes play an important role in stabilization of protein structure (Stamatakis & Papageorgiou, 1993; Papageorgiou & Murata, 1995). As shown in Figure 5, addition of sucrose stimulates V_{O_2} modestly up to a concentration of 0.9 M but sharply inhibits above 1.0 M. By contrast, between 0 and 1.2 M sucrose the half-time for photoactivation decreases monotonously from 130 to 205 s, with an average slope equal to 0.06 s/mM. These data support a model in which sucrose retards photoactivation either by increasing the solution viscosity, thereby slowing diffusion of Mn^{2+} in the bulk to its high-affinity site in the apo-WOC, or by coordination of Mn^{2+} and lowering its activity.

It is interesting that addition of 70 mM betaine, $(CH_3)_3N^+CH_2COO^-$, to the assay medium containing 300 mM sucrose leads to a modest acceleration of $t_{1/2}$ from 133 to 125 s, while also decreasing Y_{ss} by 10−15%. Moreover, the presence of 25 mM betaine in the extraction medium containing 25 mM TPDBA as chelator prevents the complete removal of manganese from PSII fragments. The residual O_2-evolving activity resulting from the addition of betaine is ~15%. It is possible that betaine, which is a zwitterionic agent known to stabilize PSII activity, does so by stabilizing protein structure against denaturation and preventing penetration of TPDBA to the WOC (Papageorgiou & Murata, 1995).

Calcium Is Essential for Reassembly of the Tetra-Mn-Ca Site. In order to determine if Ca^{2+} ions are necessary for reassembly of the tetra-Mn cluster, we studied photoactivation in the presence of sufficiently low levels of Mn^{2+} (8 μM $MnCl_2$) so that its competition with calcium reported at higher concentrations could be eliminated. Figure 6A shows that in the absence of Ca^{2+} photoactivation of TPDBA-extracted PSII membranes does not occur. The addition of 8 mM $CaCl_2$ (optimal for maximum Y_{ss}) in the dark to the same sample does not lead to immediate O_2 evolution upon pulse illumination for any dark period but instead requires

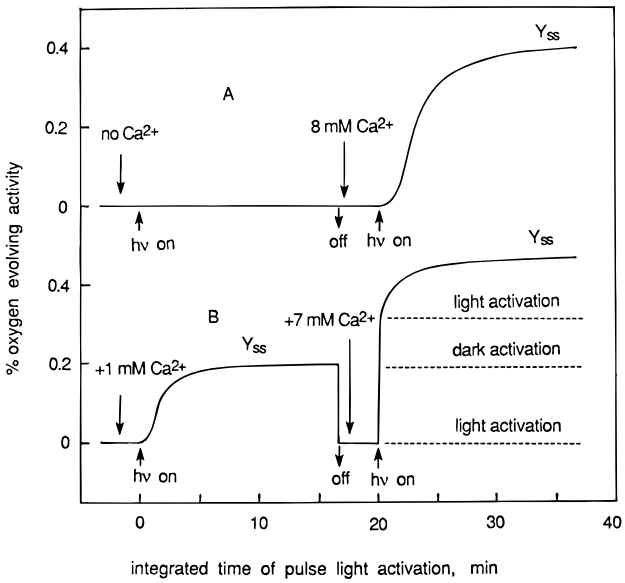

FIGURE 6: Effect of the sequential additions of Ca^{2+} on the yield of pulsed-light photoactivation in apo-PSII membranes vs the integrated light period. (A) No $CaCl_2$ is present prior to the initial pulsed-light illumination; (B) 1 mM $CaCl_2$ is present prior to the first pulsed-light exposition, followed by addition of 7 mM $CaCl_2$ in the dark before the second pulsed-light exposition. The assay and photoactivation conditions were as in Figure 1.

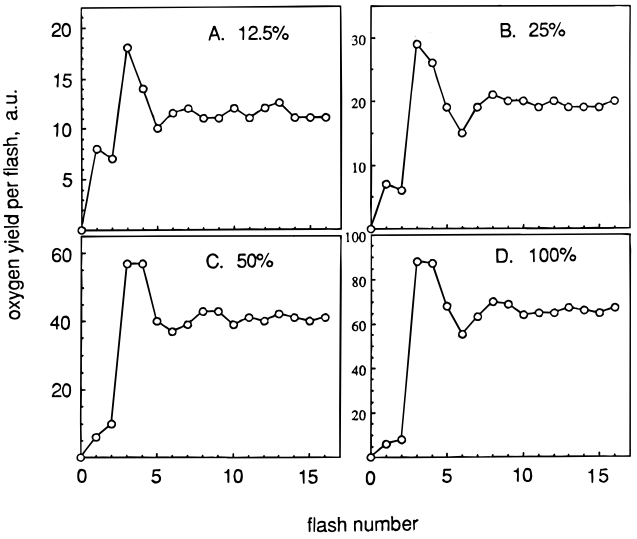

FIGURE 7: Oxygen yield per flash as a function of the number of saturating single turnover flashes (4 μs FWHM, given at 0.3 Hz) in apo-PSII upon different degrees of photoactivation achieved by pulsed-light illumination (A) after 38 light pulses or 12.5% Y_{ss}; (B) after 84 light pulses or 25% Y_{ss}; (C) after 147 light pulses or 50% Y_{ss}; (D) after 600 light pulses or 100% Y_{ss}. The parameters of pulsed-light illumination were the following: $t_{light} = 20$ ms, $t_{dark} = 1.8$ s, and $I_p = 80$ mW/cm^2. The dark period between pulsed-light photoactivation and measurement of pattern O_2 yields on saturating xenon flashes was 10 min. For other experimental details, see Materials and Methods.

an additional pulsed-light illumination with a half-time of 150−170 s which is exactly the same time as found with no prior pre-illumination at this calcium concentration (see Figure 1A). In the presence of suboptimal concentrations of Ca^{2+} (1 mM, Figure 6B) more rapid photoactivation occurs in the light to a level below the maximum Y_{ss}, and this corresponds to the half-time of 60−70 s as reported in Figure 1A. Figure 6B shows that subsequent addition of 7 mM $CaCl_2$ to this sample in the dark immediately leads to a higher Y_{ss} upon pulsed-light illumination, followed by further photoactivation to a higher maximum Y_{ss}. This result indicates that photoassembly of a metastable inactive intermediate occurs in the dark following preillumination at suboptimal concentrations of Ca^{2+} needed to produce maximal Y_{ss}. Addition of Ca^{2+} in the dark to this intermediate produces an active center without further photoactivation. In the final control experiment we found that illumination of apo-PSII in the presence of 8 mM Ca^{2+} without Mn^{2+} did not lead to photoactivation, nor did it influence the rate of photoactivation following addition of Mn^{2+}. A decrease of 3−5% in the yield of photoactivation in the presence of Mn^{2+} was found, most likely due to photoinactivation of PSII.

There are at least three possible models to consider: (a) in the absence of Ca^{2+} formation of the tetra-Mn cluster does not occur; (b) an inactive partially assembled Mn_x cluster forms, where $x = 2$ or 3, that requires ligation of Ca^{2+} in order for the remaining Mn^{2+} ions to bind and activity to be restored; (c) an inactive but assembled tetra-Mn cluster forms in the light in the absence of Ca^{2+}, but requires ligation of Ca^{2+} to restore O_2 evolution activity. According to our data, only explanation a or b could be correct. In order to distinguish between these possibilities more extensive analysis is required. Earlier studies which have used greater Mn^{2+} concentrations in order to increase the quantum yield of photoactivation are not able to eliminate model c because excess Mn^{2+} was thought to be capable of replacing Ca^{2+} in the photoassembly of inactive centers [Ono & Inoue, 1983; Miller & Brudvig, 1989; for review see Yocum (1991)]. The current data given here and those of Chen et al. (1995) indicate an absolute requirement for Ca^{2+} in photoassembly of $\{Mn_4\}$ cluster.

Pattern of O_2 Evolution on Single-Turnover Flashes. In an effort to understand if the O_2 activity of photoactivated centers changes during photoactivation, we have measured the kinetics of O_2 evolution produced by a series of saturating single turnover flashes (4 μs FWHM) at different times during recovery. Figure 7A−D show the flash pattern for O_2 formation at different times during photoactivation, between 12.5% (A), 25% (B), 50% (C), and 100% (D) of Y_{ss}. In all samples a 10 min dark pre-incubation period was used after photoactivation to establish the dark S-state populations. As seen in the figures, the characteristic four-flash oscillatory pattern for O_2 evolution is restored at all times. For comparison, Figure 8 shows the normalized O_2 yield per flash as a function of the number of single-turnover flashes for the untreated PSII membranes in the presence of 0.8 mM K_3FeCN_6. The control sample exhibits the typical period 4 oscillation pattern which has been frequently described in the literature. The following features can be inferred from Figure 7A−D: (1) for the first two flashes (Y_1 and Y_2) the high yield of O_2 evolution indicates analogous behavior to the oxidation of H_2O_2 by chemically stressed PSII membranes (Berg & Seibert, 1987; Taoka et al., 1993); (2) after the 10 min dark pre-incubation period the concentrations of the S_0/S_1 states are 50% each, which shows enhanced stability of S_1 in comparison to untreated PSII membranes (25%/75%); (3) the periodicity of oscillations is equal to 5 with the maximal O_2 evolution occurring at Y_3 and Y_8 at all levels of photoactivation, as indicated in Figure 7A−D; (4) only two periods of oscillation can be seen, indicating strong damping caused by misses; (5) the yield

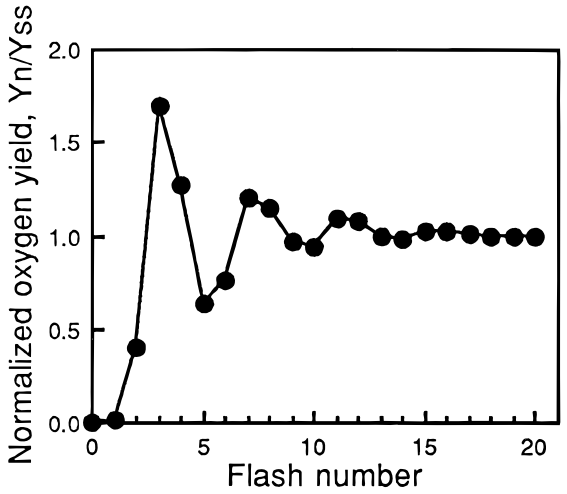

FIGURE 8: Normalized oxygen yield per flash as a function of the number of saturating single turnover flashes (4 μs FWHM, given at 0.3 Hz) in untreated BBY PSII membrane fragments after 10 min dark incubation in the presence 0.8 mM K_3FeCN_6. For other experimental details, see Materials and Methods.

at Y_2, which gives the relative concentration of the S_2-state decreases with increasing extent of photoactivation.

The ratio of the O_2 yields due to the fourth (Y_4) and the third (Y_3) flashes, Y_4/Y_3, reflecting probability of misses, α (Messinger & Renger, 1994) considerably increases with increasing level of photoactivation from 12.5% to 100%. This could indicate that the increase of α at the high level of photoactivation comprises at least two effects: one depends on the rate of deactivation of S-states, and another one reflects sample heterogeneity of the newly assembled active site of WOC.

Flash Yields from Photoactivated Centers Using Substoichiometric Mn^{2+} Concentrations. As we have previously demonstrated, the pulsed-light method of photoactivation allows O_2 detection even at substoichiometric levels of Mn^{2+} below the 4 atoms/apo-WOC required for saturation of activity. (Ananyev & Dismukes, 1995, 1996). As shown in Figure 9A, TPDBA-treated PSII could successfully reassemble a normal active WOC in the presence of as few as 1 atom of Mn^{2+}/apo-WOC ($t_{1/2} \geq 40$ min), giving maximal O_2 yield on the third flash and a few periods of oscillations. This result supports a model in which $Mn^{\geq 2+}$ can redistribute between apo-WOC centers freely. However, the ratio Y_4/Y_3 gradually increases with increasing amount of manganese from 1 to 4 Mn^{2+}/apo-WOC (Figure 9A−D). The number of oscillation periods that can be observed depend on the amount of added Mn^{2+}: for samples with 1 or 3 Mn/apo-WOC typically three to four oscillations can be distinguished. For samples with 2 or 4 Mn/apo-WOC only one or two periods of oscillations can be seen. Also, comparing Figure 7D, obtained at 8 Mn/apo-PSII, with Figure 9A−D, obtained at 1−4 Mn/apo-PSII, it is evident from the nonoscillating yield of O_2 that an increasing fraction of centers becomes scrambled (greater misses) as the Mn concentration increases. This result indicates that photoactivated centers are susceptible to higher misses in the presence of excess Mn^{2+}, presumably due to oxidation of nonfunctional Mn^{2+} in competition with water oxidation. Unlike intact PSII membranes, photoactivated samples lack the three extrinsic proteins of the WOC (17-, 23-, and 33-kDa), which accounts in part for these differences.

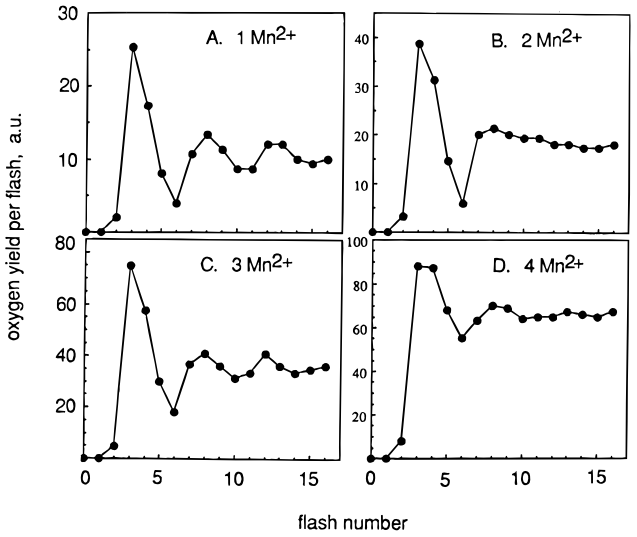

FIGURE 9: Oxygen yield per flash as a function of the number of saturating single-turnover xenon flashes (4 μs FWHM, given at 0.3 Hz) in a new reassembly holo WOC in the presence of different numbers of Mn^{2+} atoms (per apo-WOC): (A) 1 atom of Mn^{2+}; (B) 2 atoms of Mn^{2+}; (C) 3 atoms of Mn^{2+}; (D) 4 atoms of Mn^{2+}. The system was preilluminated by pulsed-light for 60, 40, 20, and 15 min, A, B, C, and D, respectively, before it reached Y_{ss}. Measurements of the O_2 evolution pattern followed a 10 min dark incubation to allow S-state equilibration. The parameters of pulsed-light illumination were $t_{light} = 20$ ms, $t_{dark} = 1.8$ s, and $I_p = 80$ mW/cm^2. For other experimental details, see Materials and Methods.

It is interesting to note that the value of Y_1 exhibits a strong dependence on the concentration of Mn^{2+} (Figures 7D and 9D). In the presence of <4 atoms of Mn^{2+}, Y_1 is markedly suppressed relative to its value with ≥4 atoms Mn^{2+}. At 1−4 Mn/apo-WOC the value of Y_1 is equal to zero. This correlation suggests that nonfunctional Mn^{2+} that is not incorporated in the $\{Mn_4\}$ cluster by photoactivation may serve to catalyze the dismutation of photogenerated hydrogen peroxide formed on Y_1 (S_2-state) by the photoactivated WOC. Note that intact PSII fragments which retain the three extrinsic proteins do not form O_2 on Y_1 (Figure 8). Hydrogen peroxide is known to form in disrupted PSII membrane fragments under conditions in which the extrinsic proteins are removed (Klimov et al., 1993) and can be detected as O_2 following dismutation. Hence, the role of the extrinsic proteins appears to include elimination of premature oxidation of water to hydrogen peroxide and protection of the $\{Mn_4\}$ cluster from aqueous reductants, including excess free Mn^{2+}.

DISCUSSION

Cations Delay the Assembly of Tetra-Mn Active Site of WOC. The data in Figures 1A and 6 clearly show that Ca^{2+} is essential for both activity of the WOC ($K_m = 1.4$ mM) and assembly of the $\{Mn_4\}$ active site but that it also greatly slows the kinetics of photoactivation at all concentrations. A 10-fold decrease in $t_{1/2}$ is measured between 1 and 40 mM Ca^{2+}. These results imply that, on the one hand, Ca^{2+} is required as an essential cofactor for supporting O_2 evolving activity [see review by Yocum (1991)] and, on the other hand, functions as an inhibitor of Mn^{2+}-dependent photoactivation. Mg^{2+} does not support O_2 evolution and is a much weaker inhibitor of Mn^{2+}-dependent photoactivation, producing less than a 50% decrease in $t_{1/2}$ from 0 to 20 mM $MgCl_2$. Consistent with data in Table 1 from Yocum (1991),

Scheme 1: Simplified Scheme for Coupling Photo-Oxidation and Deprotonation Reactions Involved in Assembly of the Tetra-Mn-Ca Active Site of WOC in the Presence of the Optimum Concentrations of Ca^{2+}, Mn^{2+}, and Cl^- Which Maximize the Photoactivation Yield, Y_{ss}[a]

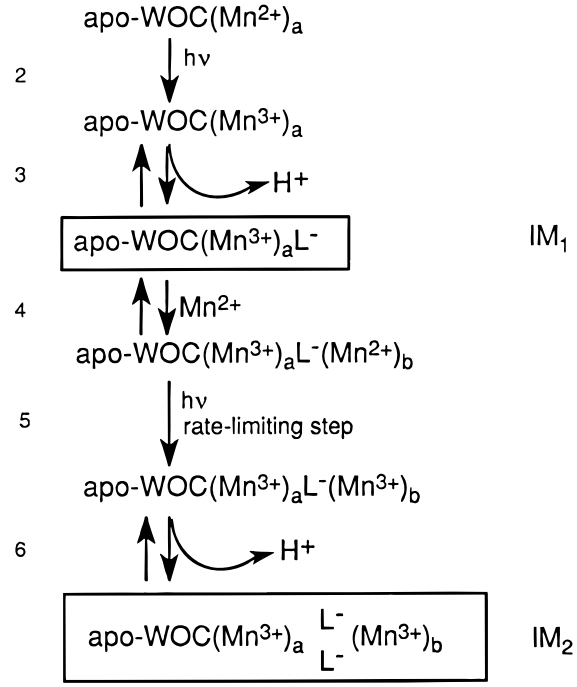

[a] $LH \leftrightarrow L^- + H^+$ designates ionization of a ligand to Mn^{3+}, either protein-derived or from water.

Mg^{2+} has no effect on Ca^{2+}-activated O_2 evolution rates in native PSII preparations. Na^+ exhibits very little influence on Mn^{2+}-dependent photoactivation. By contrast, the lanthanides, La^{3+} and Tb^{3+}, are more potent inhibitors of photoactivation ($K_m \approx 4\ \mu M$) (Ananyev et al., 1995) than of O_2 evolution in intact PSII particles ($K_1 \approx 50\ \mu M$) [reviewed in Yocum (1991) and Debus (1992)].

On the basis of these results, obtained at stoichiometric Mn concentrations (4−8 Mn^{2+}/RC) where competition with Mn at the earlier proposed Ca^{2+} binding site (Ono & Inoue, 1983) can be neglected, we suggest that cations (lanthanides^{3+}, Ca^{2+}, Mg^{2+}, Na^+) inhibit the rate of photoassembly by two distinct mechanisms. Competition for binding to one or both of the Mn specific sites involved in the first two steps of photoassembly (Scheme 1), should lead to a normal titration curve for inhibition at a specific site. The inhibition constant would depend on the affinity of the cation for the Mn^{2+} site, depending on its charge density and the size of hydration sphere. This mechanism seems to describe well the mechanism of inhibition by lanthanides and calcium. Another mechanism, electrostatic screening/attraction, is clearly indicated by the rate acceleration of photoactivation seen with TPB^-. We can expect, therefore, that water soluble cations will also exert a general electrostatic screening of negative surface charges on apo-WOC that are involved in attraction of cations to the functional Mn sites of the $\{Mn_4\}$ cluster. We propose that these surface charges on the apo-WOC complex are needed to increase the local Mn^{2+} concentration, thereby increasing the probability that assembly of a functional WOC will occur although slowing the rate of assembly through competition with other cations. Because of the low Mn concentrations found *in vivo*, this could be a physiological mechanism for ensuring assembly of active clusters. The *in vivo* competition with other cations, particularly calcium, at both types of sites would be a minor kinetic price to pay; once overcome, the assembled WOC is stable.

Special Role for Calcium in Photoactivation. It could be argued that cation screening of apo-WOC, although it lowers the local Mn^{2+} concentration, is essential for overcoming electrostatic repulsions that suppress folding of the apo-WOC into the conformation that produces stable binding of the photo-intermediates formed during photoactivation (Scheme 1). This mechanism would account for the beneficial influence on increasing the rate of photoactivation by excess Mn^{2+} concentrations that greatly exceed the concentration needed to completely load the high-affinity Mn^{2+} binding site ($K_m = 1-10\ \mu M$) (Blubaugh & Cheniae, 1992; Ghirardi & Seibert, 1996; Klimov et al., 1982).

Electrostatic steering of calcium ions by surface carboxylate groups that are not direct ligands to calcium occurs prominently in the class of calcium trigger proteins exemplified by calmodulin and calbindin (Forsen et al., 1993). The rate of binding of calcium is increased 100-fold by three carboxylate residues located within 11 Å of the calcium ions.

We believe that the essential role of Ca^{2+} in the photoactivation process consists of substituting for protons released from amino acid residues and possibly ionized water molecules that comprise the ligands to the $\{Mn_4\}$ cluster. This may possibly include one or more of the following residues of the D1 protein: Asp-59, Asp-61, Glu-62, His-92, Asp-170, His-190, His-337 [for review see Debus (1992), Preston and Seibert (1991a,b), and Chu et al. (1995)]. This leads to the formation of labile Ca^{2+}−ligand interactions having the proper conformation for photoactivation, yet still capable of substitution by $Mn^{\geq 2+}$. Competition between Ca^{2+} and Mn^{2+} in the Mn-binding site is in agreement with earlier studies (Tamura & Cheniae, 1987; Ono & Inoue, 1983; Miller & Brudvig, 1989) and the recent proposal from Cheniae's group involving structural rearrangements in the assembly of the $\{Mn_4\}$ cluster (Chen et al., 1995).

Role of Protons in Assembly of the $\{Mn_4\}$ Active Site. The data in Figure 2 demonstrate the presence of an acidic group(s) with pK = 5.4 and a basic group(s) with pK = 6.75 that must be ionized and protonated, respectively, in order to obtain maximal Y_{ss}. These results correspond closely to the results by Messinger and Renger (1994) and Kebekus et al. (1995) who found that two conformational changes of the intact WOC occur at the characteristic pH ranges between 5.3−5.6 and 6.3−6.5. In our experiments at pulsed-light illumination the narrow difference pK_2−pK_1 = 1.35 indicates that the process of reassembly of the tetra-Mn cluster in TPDBA-treated PSII membranes is very sensitive to pH. Compared to photoactivation of NaCl/NH_2OH PSII membranes or steady-state O_2 evolution by untreated PSII membranes, the analogous values of apparent ΔpK (50% inhibition points) are equal to 2.5 (Chen & Cheniae, 1995) and 2.6 (Vass & Styring, 1991), respectively. This difference between photoactivated TPDBA−PSII and untreated samples could indicate that (a) reaction of the intermediates formed in the assembly process are more sensitive to pH than the intact $\{Mn_4\}$ cluster and that (b) water soluble proteins, and 33-kDa protein in particular, provide protection of the active site of the native WOC by buffering protons from the medium.

Scheme 2: Mechanism That Explains How Deprotonation in Step 3 of Scheme 1 Might Lead to Both a Decrease in Y_{ss} and an Acceleration of the Rate of Photoactivation on the Basis of Thermodynamic Considerations[a]

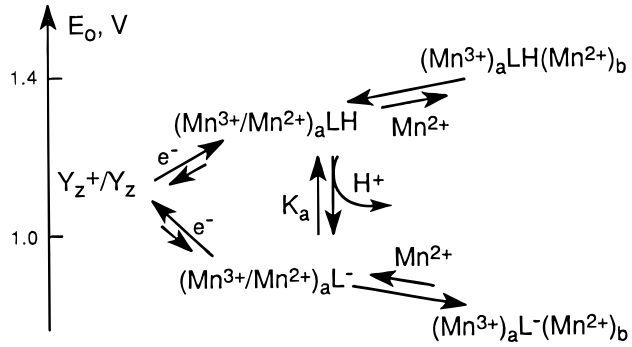

[a] The lower-potential pathway represents the thermodynamically favored reactions.

The buffer concentration effect on Y_{ss} indicates that a metastable intermediate formed in the first light-induced step prior to the rate-limiting step in photoactivation has lost one or more protons relative to the initial state prior to illumination. This deprotonation reaction can utilize buffer molecules as the proton acceptor, and so the probability that the intermediate will form and not decay by proton-induced deactivation should increase with buffer concentration. The lack of a substantial influence of the buffer concentration on $t_{1/2}$ indicates that the rate of the rate-limiting step in photoactivation does not involve release of a proton into solution. This concept is illustrated in Scheme 1 where it is shown that proton release in step 3 prior to the rate-limiting step yields a deprotonated intermediate whose steady-state concentration increases with buffering capacity. The proposed rate-limiting step in 5 involves photooxidation of the second Mn^{2+} ion and no proton release coupled to this fundamental reaction. Subsequent deprotonation of this second light-dependent intermediate is also suggested to occur analogous to step 3; however, we are unable to see this step kinetically since it follows the rate-limiting step. Hence, this second deprotonation step is conjecture based on the known 10-fold decrease in pK_a for aqua Mn^{3+} vs Mn^{2+}.

As noted above, the pK_a of the site in step 3 of Scheme 1 must be below 5.4 in order to explain the monotonic increase in the half-time (Figure 2). Unfortunately, the identity of the site is not indicated by the pK_a, as it is undoubtedly influenced by the Mn^{3+} formed. The protonation equilibrium which affects Y_{ss} (pK_a = 5.4 and 6.75) differs from the deprotonation event which affects the half-life and may even involve steps following the rate-limiting step. The pK_a values might suggest a carboxylate (5.4) perturbed by other negative charges and a histidine imidazole (6.75).

In Scheme 2 we present a thermodynamic argument that can explain how deprotonation in step 3 of Scheme 1 might lead to both a decrease in Y_{ss} and an acceleration of the rate of photoactivation. Oxidation of Mn^{2+} in the high-affinity site ("a") by Y_z^+ is known to be a reversible equilibrium reaction. The reduction potentials for hexa-aqua Mn^{3+} and Y_z^+ are indicated in Scheme 2 at 1.4 and 1.1 V. Proton loss from a ligand to photogenerated $(Mn^{3+})_a$ (formed in step 3 of Scheme 1) stabilizes the Mn^{3+} potential by an amount

$$\Delta\Delta G_a = RT \ln[1 + 10^{(pH - pK_a)}] \quad (1)$$

where this is the shift relative to the potential at low pH where the Mn ligand LH does not deprotonate (Ruttinger & Dismukes, 1996). Equation 1 predicts a 2.0 kcal/mol stabilization of the ionized form, $(Mn^{3+})_aL^-$, at pH values 2 or more units above the pK_a. By this mechanism one would predict a shift in the equilibrium between Y_z^+ and $(Mn^{2+})_a$ such that more centers will favor oxidation of $(Mn^{2+})_a$ vs Y_z upon deprotonation of ligand LH. This increase in the concentration of the first metastable intermediate, so-called IM_1, leads to an increase in the rate and yield of ligation of the second Mn^{2+} ion (site "b") noted in the second step of Scheme 2, forming the critical mixed-valent di-manganese(II,III) intermediate that is the reactant in the rate-limiting step. An increase in the concentration of this intermediate is responsible for the increase in rate of photoactivation seen in Figure 2.

In agreement with the first step of the model, steady-state measurements performed on core complexes and Tris-treated PSII membranes show that the apparent K_M value for the reaction, Mn^{2+} → apo-PSII → DCIP, is strongly pH-dependent (Tamura et al., 1991; Magnuson & Andréasson, 1995). This could be due to the dissociation of Mn^{2+} arising from its weaker binding affinity at site "a" vs Mn^{3+}.

Characteristics of the Flash Yield Kinetics of O_2 Evolution. The illumination of PSII fragments by a saturating xenon flash excites all centers [for review see Joliot and Kok (1975)], so that all events occur stepwise and provide uniformity to the system if a homogeneous dark population pre-exists. The basic features of the flash experiments performed on photoactivated apo-WOC (Figures 7 and 9) demonstrate that (a) a higher concentration of S_1- than S_0-state exists relative to untreated PSII; (b) the periodicity close to 4 and multiple oscillation patterns seen with 1 or 3 Mn/apo-WOC shows that photoactivated WOC centers lacking excess nonfunctional Mn^{2+} have the same basic misses, α, and double hits, β, as do intact PSII centers; (c) an increased damping of oscillations seen with 2 or 4 Mn^{2+} atoms/apo-WOC indicates that additional misses occur; (d) at sub-stoichiometric Mn levels in the medium there is redistribution between partially assembled inactive centers and fully assembled tetra-Mn-Ca active centers.

ACKNOWLEDGMENT

We are grateful to L. Zaltsman for her help in preparation of this article and to Dr. A. E. M. Boelrijk for performing measurements of TPB redox potential. Mr. Daniel Katz and Professors G. W. Brudvig, G. M. Cheniae, V. V. Klimov, and A. W. Rutherford have provided useful advice.

REFERENCES

Ädelroth, P., Lindberg, K., & Andréasson, L.-E. (1995) *Biochemistry 34*, 9021−9027.

Ananyev, G. M., & Dismukes, G. C. (1995) in *Photosynthesis: From Light to Biosphere* (Mathis, P., Ed.) Vol. 2, pp 431−434, Kluwer Academic Publishers, Dordrecht, The Netherlands.

Ananyev, G. M., & Dismukes, G. C. (1996) *Biochemistry 35*, 4102−4109.

Ananyev, G. M., Bruntrager, E., & Dismukes, G. C. (1995) *Photosynth. Res.* (Suppl. 1), p 98 P-7−050.

Berg, S. P., & Seibert, M. (1987) *Photosynth. Res. 13*, 3−17.

Berthold, D. A., Babcock, G. T., & Yocum, C. F. (1981) *FEBS Lett. 134*, 231−234.

Blubaugh, D. J., & Cheniae, G. M.(1992) in *Research in Photosynthesis* (Murata, N., Ed.) Vol. 2, pp 361−364, Kluwer Academic Publishers, Dordrecht, The Netherlands.
Boussac, A., & Rutherford, A. W. (1988) *Biochemistry 27*, 3476−3483.
Boussac, A., Zimmerman, J., & Rutherford, A. W. (1989) *Biochemistry 28*, 8984−8989.
Chen, C., & Cheniae, G. M. (1995) in *Photosynthesis: From Light to Biosphere* (Mathis, P., Ed.) Vol. 2, pp 329−332, Kluwer Academic Publishers, Dordrecht, The Netherlands.
Chen, C., Kazimir, J., & Cheniae, G. M. (1995) *Biochemistry 34*, 13511−13526.
Cheniae, G. M. (1980) *Methods Enzym. 69*, 349−363.
Chu, H.-A., Nguen, A. P., & Debus, R. J. (1995) *Biochemistry 34*, 5839−5858.
Debus, R. J. (1992) *Biochim. Biophys. Acta 1102*, 269−353.
Erixon, K., & Renger, G. (1974) *Biochim. Biophys. Acta 333*, 95−106.
Fleweling, R., & Hubbell, W. (1986) *Biophys. J. 49*, 541−552.
Forsen, S., Kordel, J., Grundstrom, T., & Chazin, W. J. (1993) *Acc. Chem. Res. 26*, 7−14.
Ghanotakis, D. F., Babcock, G. T., & Yocum, C. F. (1984) *Biochim. Biophys. Acta 765*, 388−398.
Ghirardi, M. L., & Seibert, M. (1996) *Biochemistry 35*, 1820−1828.
Hatch, C., Grush, M., Bradley, R., LoBrutto, R., Cramer, S., & Frash, W. (1995) in *Photosynthesis: From Light to Biosphere* (Mathis, P., Ed.) Vol. 2, pp 425−429, Kluwer Academic Publishers, Dordrecht, The Netherlands.
Itoh, S., Tamura, N., Hashimoto, K., & Nishimura, M. (1983) in *The Oxygen Evolving System of Photosynthesis* (Inoue, Y., et al., Eds.) pp 421−430, Academic Press Japan, Tokyo, Japan.
Johnson, G. N., Rutherford, A. W., & Krieger, A. (1995) *Biochim. Biophys. Acta 1229*, 202−207.
Joliot, P., & Kok, B. (1975) in *Bioenergetics of Photosynthesis* (Govindjee, Ed.), pp 387−412, Academic Press, New York.
Kebekus, U., Messinger, J., & Renger, G. (1995) *Biochemistry 34*, 6175−6182.
Khanna, R., Rajan, S., Govindjee, & Gutowsky, H. S. (1981) in *Photosynthesis II. Electron Transport and Photophosphorylation* (Akoyunoglou, G., Ed.), pp 307−316, Balaban Int. Science Services, Philadelphia, PA.
Klimov, V. V., Allakhverdiev, S. I., Shuvalov, V. A., & Krasnovsky, A. A. (1982) *Dokl. Akad. Nauk SSSR 263*, 1001−1007.
Klimov, V. V., Ananyev, G. M., Allakhverdiev, S. I., Zharmukhamedov, S. K., Mulay, M., Hedge, U., & Padhy, S. (1990) in *Current Research in Photosynthesis* (Baltscheffsky, H., Ed.) Vol. 1, pp 247−254, Kluwer Academic Publishers, Dordrecht, The Netherlands.
Klimov, V. V., Ananyev, G. M., Zastryzhnaya, O. Wydrzynski, T., & Renger, G. (1993) *Photosynth. Res. 38*, 409−416.
Latimer, M. J., DeRose, V. J., Mukerji, I., Yachandra, V. K., Sauer, K., & Klein, M.P. (1995) *Biochemistry 34*, 10898−10909.
Magnuson, A., & Andréasson, L.-E. (1995) in *Photosynthesis: from Light to Biosphere* (Mathis, P., Ed.) Vol. 2, pp 393−396, Kluwer Academic Publishers, Dordrecht, The Netherlands.
Messinger, J., & Renger, G. (1994) *Biochemistry 33*, 10896−10905.
Miller, A.-F., & Brudvig G. (1989) *Biochemistry 28*, 8181−8190.
Miyao, M., & Inoue, Y. (1991) *Biochim. Biophys. Acta 1056*, 47−56.
Miyao-Tokutomi, M., Ono, T.-A., & Inoue, Y. (1990) in *Current Research in Photosynthesis* (Baltscheffsky, H., Ed.) Vol. 1, pp 909−912, Kluwer Academic Publishers, Dordrecht, The Netherlands.
Mizusawa, N., & Yamashita, T. (1992) in *Research in Photosynthesis* (Murata, N., Ed.) Vol. 2, pp 425−428, Kluwer Academic Publishers, Dordrecht, The Netherlands.
Mizusawa, N., & Yamashita, T. (1995) in *Photosynthesis: from Light to Biosphere* (Mathis, P., Ed.) Vol. 2, pp 531−534, Kluwer Academic Publishers, Dordrecht, The Netherlands.
Mizusawa, N., Ebina, M., & Yamashita, T. (1995) *Photosynth. Res. 45*, 71−77.
Noguchi, T., Ono, T.-A., & Inoue, Y. (1995) *Biochim. Biophys. Acta 1228*, 189−200.
Ono, T.-A., & Inoue, Y. (1983a) *Biochim. Biophys. Acta 723*, 191−201.
Ono, T.-A., & Inoue, Y. (1983b) in *The Oxygen Evolving System of Photosynthesis* (Inoue, Y., et al., Eds.) pp 337−344, Academic Press Japan, Tokyo, Japan.
Papageorgiou, G. C., & Murata, N. (1995) *Photosynth. Res. 44*, 243−252.
Preston, C., & Seibert, M. (1991a) *Biochemistry 30*, 9615−9624.
Preston, C., & Seibert, M. (1991b) *Biochemistry 30*, 9625−9633.
Radmer, R., & Cheniae, G. M. (1971) *Biochim. Biophys. Acta 253*, 182−186.
Radmer, R., & Cheniae, G. M. (1977) in *Primary Processes of Photosynthesis* (Barber, J., Ed.) Vol. 2, pp 303−348, Elsevier, Amsterdam, The Netherlands.
Riggs-Gelasco, P. J., Yocum, C. F., & Penner-Hahn, J. E. (1995) *Inorg. Biochem. 59*, 616.
Ruttinger, W., & Dismukes, G. C. (1996) *Chem. Rev.* (submitted for publication).
Stamatakis, C., & Papageorgiou, C. (1993) *Biochim. Biophys. Acta 1183*, 333−338.
Tamura, N., & Cheniae, G. M. (1987) *Biochim. Biophys. Acta 890*, 179−194.
Tamura, N., & Cheniae, G. M. (1988) in *Light-Energy Transduction in Photosynthesis: Higher Plants and Bacterial Models* (Stevens, S. E., & Bryant, D. A., Eds.) pp 227−242, The American Society of Plant Physiologists, Rockville, MD.
Tamura, N., Kamachi, H., Hokari, N., Masumoto, H., & Inoue, H. (1991) *Biochim. Biophys. Acta 1060*, 51−58.
Tamura, N., Tanaka, T., Wakamatsu, K., Inoue, H., & Wada, K. (1992) in Research in Photosynthesis (Murata, N., Ed.) Vol. 2, pp 405−408, Kluwer Academic Publishers, Dordrecht, The Netherlands.
Taoka, S., Jursinic, P. A., & Seibert, M. (1993) *Photosynth. Res. 38*, 425−431.
Tso, J., Sivaraja, M., & Dismukes, G. C. (1991) *Biochemistry 30*, 4734−4739.
Vass, I., & Styring, S. (1991) *Biochemistry 30*, 830−839.
Yachandra, V. K., DeRose, V. J., Latimer, M. J., Mukerji, I., Sauer, K., & Klein, M.P. (1993) *Science 260*, 675−679.
Yocum, C. F. (1991) *Biochim. Biophys. Acta 1059*, 1−15.

BI960894T